Analysis of Cloud Water Resources over Fuxin Region

Ke SUN, Ning LI, Yuan XIE, Xiaotong YANG, Haiyan SHU*, Xu ZHANG, Xilong NING
Fuxin Meteorological Bureau, Fuxin 123000, China

Abstract Based on the data of microwave radiometers, GPS/MET, and ERA5 from Fuxin Mongolian Autonomous County in Liaoning Province, the changing characteristics of atmospheric water vapor and liquid water in Fuxin City during 2020 – 2021 were analyzed. The results show that during the typical precipitation processes, the variation trends of integrated cloud liquid water content were basically consistent with those of precipitation. The statistical analysis of distribution laws of integrated atmospheric water vapor content and integrated liquid water content in clouds at different precipitation levels 1 h before the precipitation had obvious guiding significance for improving the scientific operation ability of artificial precipitation enhancement operations. The integrated water vapor content and integrated liquid water content in clouds before the onset of precipitation rose with the increase of precipitation intensity from light rain to rainstorms. The evolution characteristics of atmospheric total water vapor content and integrated liquid water content during 33 precipitation processes reveal that the variation rates of atmospheric total water vapor content and integrated liquid water content 1 and 3 h before the precipitation averaged 0.42 and 5.05, respectively. Before the precipitation, the total water vapor content and integrated liquid water content in clouds peaked and then decreased briefly. From their sudden increases to the beginning of the precipitation, there was an advance of about 30 – 50 min, and the possibility of precipitation was high, which can be one of the indicators of precipitation occurrence.
Key words Cloud water resources; Artificial precipitation enhancement; Microwave radiometer
DOI 10.19547/j.issn2152 – 3940.2026.04.008

Fuxin City is located in the transition zone between the Inner Mongolia Plateau and Liaodong Plain in Northeast China, with an annual mean precipitation of below 500 mm. Here, water resources are scarce, and the seasonal distribution of precipitation is uneven. The cloud water resources in the air are one of the main sources of water resources for agricultural production in Fuxin. Artificial precipitation enhancement is an important measure for agricultural drought mitigation and disaster reduction in Fuxin. Therefore, accurately analyzing the changing patterns of cloud water resources in Fuxin is of great significance for scientifically conducting artificial precipitation enhancement operations to resist agricultural drought. At present, many meteorological researchers have conducted a series of analyses of the distribution of atmospheric water vapor in different regions and have achieved many practical scientific research results[1 – 6]. In this paper, based on the meteorological data of ground-based microwave radiometers, GPS/MET, and ERA5 from Fuxin Mongolian Autonomous County in Liaoning Province, the changing characteristics of cloud water resources in Fuxin City from 2020 to 2021 were analyzed to provide scientific support for artificial precipitation enhancement operations.

1 Sources of data and methods

Based on the meteorological observation data of GPS/MET and microwave radiometers in Fuxin Mongolian Autonomous County (54237) from 2020 to 2021, as well as ERA5 reanalysis data, the changes in atmospheric water vapor in Fuxin City were analyzed to provide scientific operational guarantees for artificial precipitation enhancement. The meteorological observation data mainly included the data of precipitable water vapor (PWV), atmospheric water vapor content, liquid water content in clouds, temperature, relative humidity, precipitation, and cloud cover.

The atmospheric water vapor products of GPS/MET, microwave radiometers, and ERA5 reanalysis data were compared and analyzed. The practical performance of the data was evaluated using average error, root mean square error, and correlation coefficient. The monthly and daily changes of atmospheric water vapor content were analyzed. Statistical analysis methods were used to analyze the temporal distribution and vertical variations of atmospheric water vapor products.

2 Results and analysis

2.1 Temporal changes of atmospheric water vapor The temporal changes of integrated cloud liquid water content before and after precipitation were analyzed, and the relationship between the changes in hourly precipitation and integrated cloud liquid water content in 6 precipitation processes from April to September during 2020 – 2021 was discussed. As shown in Fig. 1, the changing trend of integrated cloud liquid water content was basically consistent with that of precipitation. At 15:00 on April 22, 2021, integrated cloud liquid water content was relatively small, and that of microwave radiometers and ERA5 was 0.178 and 0.185 mm, respectively, while hourly precipitation was 0 mm (Fig. 1a). At 16:00, that of microwave radiometers and ERA5 was 0.155 and 0.265 mm, respectively, while hourly precipitation was still

Received: February 18, 2026 Accepted: April 20, 2026
Supported by the Science and Technology Achievement Project of Liaoning Meteorological Bureau (ZD202527).
* Corresponding Author.

0 mm. Integrated cloud liquid water content increased rapidly from 17:00 to 18:00, reaching the maximum (microwave radiometers: 1.785 mm, ERA5: 1.954 mm) at 19:00, and hourly precipitation also peaked, up to 0.6 mm. At 21:00, the integrated liquid water content and hourly precipitation both slightly decreased. After the precipitation ended at 23:00, integrated cloud liquid water content rapidly dropped to below 0.2 mm. As the precipitation began at 01:00 on April 23, integrated cloud liquid water content rose again, and that of microwave radiometers and ERA5 increased to 2.129 and 2.029 mm at 07:00, while hourly precipitation was 1.1 mm. With the end of precipitation at 20:00, integrated cloud liquid water content rapidly decreased to around 0.2 mm.

At 05:00 on July 13, 2021 (Fig. 1d), integrated cloud liquid water content was below 0.2 mm. Before the precipitation began, integrated cloud liquid water content rose above 1.0 mm. At 08:00, the precipitation started, and integrated cloud liquid water content increased. That of microwave radiometers and ERA5 rose to 2.838 and 1.85 mm, respectively, and hourly precipitation was 0.5 mm. At 14:00, hourly precipitation reached the maximum (7.7 mm), and integrated cloud liquid water content increased to 12.403 mm for microwave radiometers and 13.153 mm for ERA5. At 15:00, the precipitation showed a pause, and integrated cloud liquid water content dropped below 1 mm. At 17:00, integrated cloud liquid water content remained above 3.0 mm as the precipitation continued. At 09:00, hourly precipitation was the largest, up to 6.5 mm, and integrated cloud liquid water content reached 12.047 mm for microwave radiometers and 11.126 mm for ERA5. At 23:00, hourly precipitation began to decrease again until 02:00 on April 14. At 06:00, hourly precipitation was up to 7 mm, integrated cloud liquid water content was 11.820 mm for microwave radiometers and 12.340 mm for ERA5. At 09:00, the precipitation ended, and the liquid water content dropped below 0.5 mm.

From Fig. 1, it can be seen that before the precipitation began, there was a significant increase in integrated cloud liquid water content, and the precipitation cloud system was in the development stage. Seizing the favorable opportunity to carry out artificial precipitation enhancement operations could accelerate the occurrence of precipitation and was also beneficial for increasing total precipitation. Integrated cloud liquid water content was positively correlated with precipitation. That is, their peaks, troughs and brief drops during the precipitation process were consistent. As the precipitation continued, integrated cloud liquid water content was basically above 2.0 mm. After the precipitation ended, integrated cloud liquid water content rapidly dropped to below 1.0 mm. Therefore, integrated cloud liquid water content can better indicate the distribution pattern of precipitation, which has a significant indication effect on artificial precipitation enhancement operations.

2.2 Analysis of water vapor content and liquid water content at different precipitation levels Based on 50 precipitation cases in Fuxin Mongolian Autonomous County, Liaoning Province from April to September in 2020 and 2021, the integrated water vapor content and integrated liquid water content in clouds 1 h before the precipitation, as well as the weather conditions, were statistically analyzed (Table 1). Before the occurrence of rainstorms, integrated cloud liquid water content exceeded 5.7 mm, and the integrated water vapor content surpassed 6.4 cm. Before the occurrence of heavy rain, integrated cloud liquid water content was above 5.0 mm, and the integrated water vapor content was more than 5.1 cm. Before the occurrence of moderate rain, integrated cloud liquid water content ranged from 3.9 to 4.9 mm, and the integrated water vapor content varied from 4.0 to 5.7 cm. During light rain processes, integrated cloud liquid water content was between 0.7 and 2.8 mm, and the integrated water vapor content was 2.0 – 4.7 cm. In general, the integrated water vapor content and integrated liquid water content in clouds rose with the increase of precipitation intensity.

2.3 Changing characteristics of atmospheric total water vapor content and integrated liquid water content before and after the precipitation Based on the data of atmospheric total water vapor content (V) and integrated liquid water content (L) observed by microwave radiometers, as well as the data of precipitation from ground automatic observation stations during 33 precipitation weather processes from April to September in 2020 and 2021, the evolution characteristics of V and L before and after the precipitation were analyzed. Meanwhile, the changing rates of V and L 1 and 3 h before the precipitation were calculated according to the following formulas: $f_V = (V_1 - V_3)/V_3$, $f_L = (L_1 - L_3)/L_3$, where f_V and f_L are the changing rates of V and L; V_1 and L_1 are the total water vapor content and integrated liquid water content 1 h before the precipitation; V_3 and L_3 are the total water vapor content and integrated liquid water content 3 h before the precipitation. Besides, the changing characteristics of V and L before and after precipitation were explored.

As shown in Table 2, the average of V 3 h before the precipitation was 30.84 mm. As the precipitation process approached, V increased significantly. The average of V 1 h before the precipitation was up to 44.24 mm, and the average of f_V was 0.42. Similarly, the change of L before the precipitation was also quite obvious. The averages of L 1 and 3 h before the precipitation were 4.78 and 0.81 mm, and the average of f_L was 5.05. Within 3 h before the precipitation, the change of L was greater than that of V, and f_L was much larger than f_V, indicating that the integrated liquid water content changed more significantly before the precipitation began. During the precipitation process on August 17, 2020, V and L reached 73.5 and 5.12 mm 1 h before the precipitation began, and f_V and f_L were 1.07 and 18.69, respectively. During the precipitation process on June 24, 2021, V and L were up to 42.4 and 2.52 mm 1 h before the precipitation began, and f_V and f_L were 0.86 and 3.58, respectively. In all precipitation cases, the averages of V and L 1 h after the precipitation ended were 31.46 and 0.70 mm, and the averages of V and L 3 h after the precipitation ended were 28.00 and 0.33 mm, which were almost all lower than the background values of V and L 3 h before the precipitation. This indicates that V and L decreased significantly after the precipitation ended, and the change of L was greater than that of V. During the precipitation process, liquid water in clouds formed raindrops and fell to the ground, resulting in a significant reduction in the liquid water content in the air and the atmospheric water vapor content after the precipitation ended. Before the precipitation occurred, the monitoring results of the radiometers show that both the water vapor content and integrated liquid water content reached peaks and then dropped briefly. From the sudden increases of V and L to the start of the precipitation, there was an advance of about 30 – 50 min. The rapid increase of V and L indicated the rapid aggregation of water vapor above the observation stations, and the possibility of precipitation was high, which could be one of the indicators of precipitation occurrence.

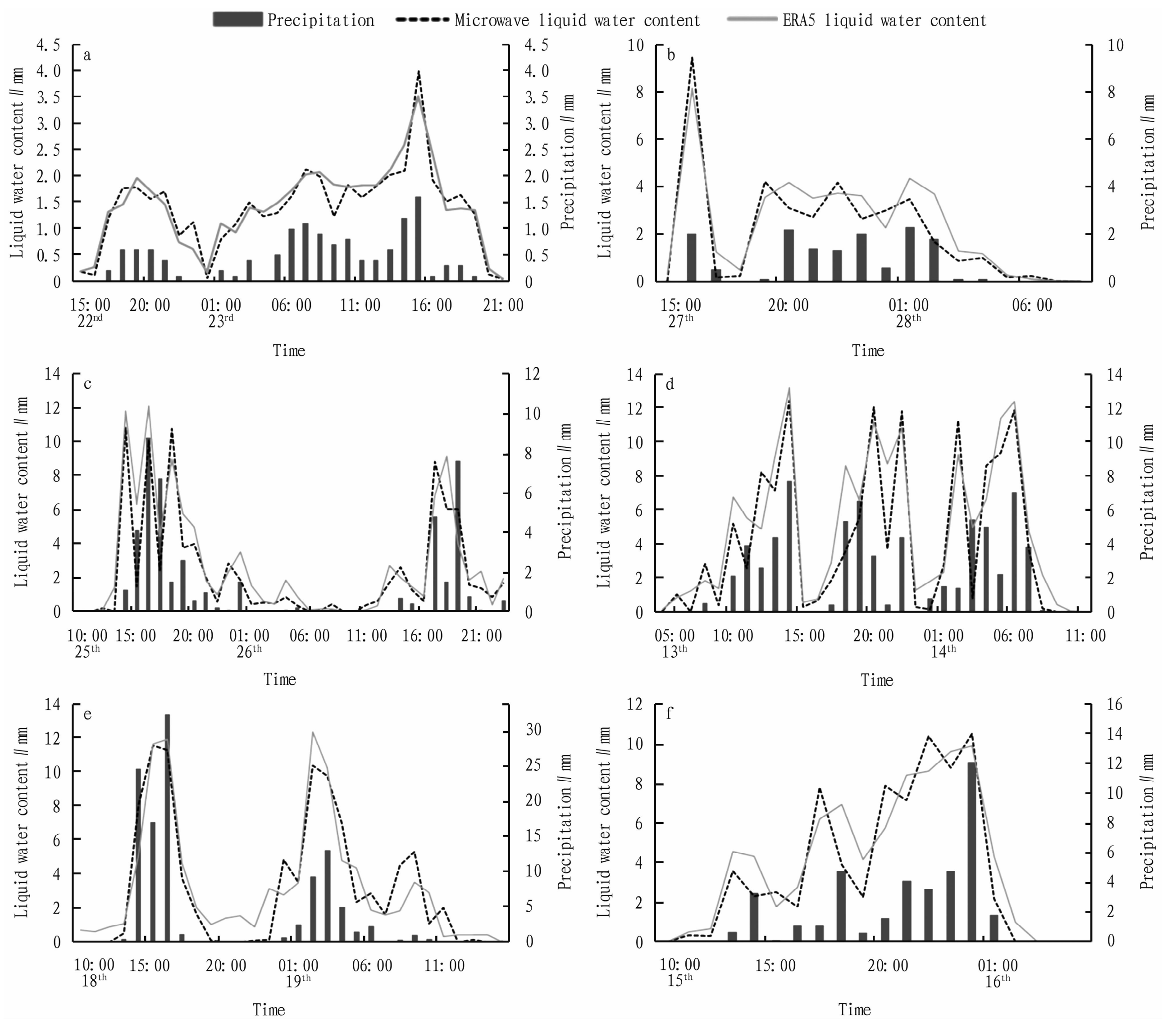

Note: a. April 2021; b. May 2021; c. June 2021; d. July 2021; e. August 2020; f. September 2020.

Fig. 1 Changes in precipitation and liquid water content from microwave radiometers and ERA5 during 6 precipitation processes in 2020 and 2021

Table 1 Integrated water vapor content and integrated liquid water content in clouds at different precipitation levels in 2020 and 2021

Year	Date	Integrated liquid water content // mm	Integrated water vapor content // cm	Weather condition	Year	Date	Integrated liquid water content // mm	Integrated water vapor content // cm	Weather condition
2020	08 – 18	7.4	8.4	Rainstorm	2021	08 – 09	4.3	4.1	Moderate rain
2020	08 – 24	7.1	6.4	Rainstorm	2021	08 – 20	4.0	4.6	Moderate rain
2021	09 – 20	5.7	9.4	Rainstorm	2021	08 – 21	4.0	4.0	Moderate rain
2020	05 – 31	5.7	6.3	Heavy rain	2021	09 – 06	4.3	4.5	Moderate rain

(To be continued)

(Continued)

Year	Date	Integrated liquid water content//mm	Integrated water vapor content//cm	Weather condition	Year	Date	Integrated liquid water content//mm	Integrated water vapor content//cm	Weather condition
2020	08-13	6.2	8.4	Heavy rain	2021	09-21	4.9	4.1	Moderate rain
2020	08-19	5.4	7.0	Heavy rain	2021	09-27	3.9	4.1	Moderate rain
2020	08-27	5.1	6.2	Heavy rain	2020	04-17	2.6	4.3	Light rain
2020	09-05	8.2	5.8	Heavy rain	2020	04-20	1.8	3.8	Light rain
2020	09-15	4.9	5.5	Heavy rain	2020	07-03	2.4	3.8	Light rain
2021	06-25	5.1	5.7	Heavy rain	2020	07-14	1.1	3.8	Light rain
2021	07-03	5.4	5.1	Heavy rain	2020	08-12	1.3	4.7	Light rain
2021	07-13	5.4	5.2	Heavy rain	2020	08-17	1.0	4.3	Light rain
2021	07-14	5.8	6.1	Heavy rain	2020	09-09	1.4	2.9	Light rain
2020	07-05	4.0	5.7	Moderate rain	2021	04-12	1.1	2.1	Light rain
2020	07-29	3.9	4.1	Moderate rain	2021	04-22	1.5	3.3	Light rain
2020	08-02	4.6	4.1	Moderate rain	2021	05-06	0.7	1.9	Light rain
2020	08-03	4.0	4.3	Moderate rain	2021	05-23	1.5	2.4	Light rain
2020	09-16	4.3	4.1	Moderate rain	2021	05-27	1.2	3.1	Light rain
2021	06-02	3.9	4.3	Moderate rain	2021	06-12	2.4	3.3	Light rain
2021	06-15	4.0	4.0	Moderate rain	2021	06-14	1.7	4.4	Light rain
2021	06-17	4.1	4.8	Moderate rain	2021	06-24	2.6	2.8	Light rain
2021	06-21	4.6	4.2	Moderate rain	2021	07-08	2.8	3.7	Light rain
2021	06-26	4.2	4.7	Moderate rain	2021	08-01	2.3	4.9	Light rain
2021	07-30	4.5	5.5	Moderate rain	2021	08-11	2.3	4.3	Light rain
2021	07-31	4.1	4.9	Moderate rain	2021	09-08	2.2	3.7	Light rain

Table 2 Changes in V and L before and after the precipitation

Year	Date	3 h before the precipitation		1 h before the precipitation				1 h after the precipitation		3 h after the precipitation	
		V//mm	L//mm	V//mm	L//mm	f_V	f_L	V//mm	L//mm	V//mm	L//mm
2020	05-31	20.10	0.15	30.80	1.12	0.53	6.47	17.50	0.170	15.8	0.021
2020	07-03	32.70	0.45	49.80	2.11	0.52	3.69	33.90	0.080	32.5	0
2020	07-05	33.60	0.52	38.80	1.17	0.15	1.25	33.50	0.180	30.6	0
2020	07-14	30.70	1.13	36.00	3.21	0.17	1.84	33.40	0.025	31.5	0
2020	08-02	35.70	1.55	49.00	4.64	0.37	1.99	38.00	0.590	34.9	0.190
2020	08-03	32.90	1.29	39.70	4.34	0.21	2.36	49.20	0.610	34.2	0
2020	08-12	39.70	0.37	42.00	3.14	0.06	7.49	44.20	0.039	43.5	0
2020	08-13	34.20	0.25	63.50	3.69	0.86	13.76	46.10	0.270	37.1	0
2020	08-17	35.50	0.26	73.50	5.12	1.07	18.69	48.60	0.015	48.1	0
2020	08-18	38.10	0.32	47.30	2.22	0.24	5.94	43.90	0.025	42.2	0.017
2020	09-05	29.50	0.86	57.30	2.51	0.95	1.92	26.10	0.215	23.8	0
2020	09-09	29.80	0.31	31.90	0.75	0.07	1.42	26.70	0.170	26.6	0.110
2020	09-15	26.90	0.53	30.20	2.15	0.12	3.06	22.30	0.110	16.7	0
2021	04-12	18.30	0.53	21.00	1.41	0.14	1.66	12.40	0.190	9.0	0.007
2021	04-22	19.50	0.64	21.20	1.53	0.08	1.39	34.90	1.520	25.1	0.500
2021	05-06	14.10	0.90	16.50	2.44	0.17	1.71	9.90	0.027	8.1	0.001
2021	05-23	20.50	0.48	23.30	1.32	0.14	1.75	9.50	0.071	8.1	0.002
2021	05-27	16.60	0.65	19.20	1.91	0.15	1.94	18.30	0.590	14.1	0.077
2021	06-02	30.60	0.92	43.90	3.22	0.43	2.50	23.80	0.460	10.7	0.028
2021	06-12	26.00	0.89	32.90	2.41	0.26	1.71	20.60	0.130	18.9	0.013
2021	06-21	21.30	0.13	23.80	0.32	0.12	1.46	23.90	0.100	21.7	0
2021	06-24	22.80	0.55	42.40	2.52	0.86	3.58	23.90	0.180	21.6	0
2021	06-25	30.10	0.15	38.30	1.10	0.27	6.33	31.40	0.670	31.1	0.460
2021	07-03	32.40	0.43	37.30	0.78	0.15	0.81	31.70	0.350	30.3	0.140
2021	07-08	31.40	0.56	49.70	3.74	0.58	5.68	33.40	0.080	31.9	0
2021	07-13	45.80	0.26	62.60	2.56	0.37	8.85	43.20	0.052	42.1	0.093

(To be continued)

(Continued)

Year	Date	3 h before the precipitation		1 h before the precipitation				1 h after the precipitation		3 h after the precipitation	
		V//mm	L//mm	V//mm	L//mm	f_V	f_L	V//mm	L//mm	V//mm	L//mm
2021	08-01	50.60	3.50	58.20	12.78	0.15	2.65	45.90	3.700	41.4	1.910
2021	08-09	35.40	1.03	94.10	23.05	1.66	21.38	41.10	2.190	40.6	1.340
2021	08-20	42.60	1.85	55.20	9.74	0.29	4.26	45.10	2.900	41.0	1.390
2021	09-06	42.70	1.93	73.90	32.91	0.73	16.05	39.80	2.830	38.0	1.710
2021	09-08	30.40	0.55	68.10	2.52	1.24	3.58	33.20	0.760	30.5	0.570
2021	09-09	36.40	1.37	56.10	12.70	0.54	8.27	30.90	2.610	28.1	2.130
2021	09-27	30.40	1.29	32.70	2.72	0.08	1.11	22.30	1.070	14.2	0.120
Average		30.84	0.81	44.24	4.78	0.42	5.05	31.46	0.700	28.0	0.330

3 Conclusions and discussion

(1) During the 6 typical precipitation processes, the variation trends of integrated cloud liquid water content were basically consistent with that of precipitation. From the statistical analysis of 50 different precipitation cases, the distribution laws of integrated atmospheric water vapor content and integrated liquid water content in clouds at different precipitation levels 1 h before the precipitation were obtained. The discriminant indicators for agricultural drought mitigation and precipitation enhancement operations were established, which had obvious guiding significance for improving the scientific operation ability of artificial precipitation enhancement operations in Fuxin City.

(2) The integrated water vapor content and integrated liquid water content in clouds before the onset of precipitation rose with the increase of precipitation intensity from light rain to rainstorms.

(3) Based on the data of atmospheric total water vapor content and integrated liquid water content observed by microwave radiometers during 33 precipitation processes, their evolution characteristics were analyzed. The results show that the averages of f_V and f_L 1 and 3 h before the precipitation were 0.42 and 5.05, respectively. Before the precipitation appeared, the total water vapor content and integrated liquid water content in clouds peaked and then declined briefly. From the sudden increases of V and L to the beginning of the precipitation, there was an advance of about 30-50 min. The rapid increase of V and L indicated that the possibility of precipitation was high, which could be one of the indicators of precipitation occurrence.

References

[1] ZHOU LD, ZHANG HX. 3D Ground-based GNSS water vapor tomography optimization using ERA-Interim reanalysis product[J]. Journal of Geodesy and Geodynamics, 2018, 38(2): 195-199.

[2] LI GW, AO J, XING FH, *et al.* Research on the characteristics of temporal and spatial distribution of precipitable water in Hainan Island based on NVAP-M and ERA-I data[J]. Torrential Rain and Disasters, 2018, 37(3): 281-287.

[3] MO ZX, HUANG L, GUO X, *et al.* Accuracy of ERA5 reanalysis data in retrieving GNSS precipitable water vapor over Guilin[J]. Journal of Nanjing University of Information Science & Technology, 2021, 13(2): 131-137.

[4] ZHANG SQ, GUO YJ, WANG GF. A comparative study of atmospheric humidity over China between radiosonde and the third generation reanalysis datasets[J]. Acta Meteorologica Sinica, 2018, 76(2): 289-303.

[5] MA XQ, ZHANG XJ, MA YY, *et al.* Comparative analysis of multisource water vapor data in three river source and nearby areas[J]. Plateau Meteorology, 2019, 38(1): 78-87.

[6] LI JX, LI PR, JIN LJ, *et al.* Remote sensing of precipitable water vapor features and application in precipitation analysis by using ground-based microwave radiometer[J]. Journal of Arid Meteorology, 2017, 35(5): 767-775.

Acknowledgement

Meteorological and Environmental Research [ISSN: 2152-3940] is a comprehensive meteorological and environmental scientific journal, and contains strong technicality and high orientation in China, being published bimonthly in Rhode Island, USA. It has been included by UPD, Chemical Abstracts, CABI, Cambridge Scientific Abstracts, EBSCO, AGRIS, EA, Chinese Science and Technology Periodical Database, Library of Congress (United States), and CNKI.

Fortunately, for the contributions of all authors and readers to *Meteorological and Environmental Research*, it has been published successfully for sixteen years. And we, all members of the editor office of *Meteorological and Environmental Research*, appreciate all help and assistance from you in the publication of our journal.